Environ Biol Fish (2022) 105:2065–2082
https://doi.org/10.1007/s10641-022-01273-1

Quantifying the effects of tides, river flow, and barriers on movements of Chinook Salmon smolts at junctions in the Sacramento – San Joaquin River Delta using multistate models

Michael J. Dodrill · Russell W. Perry · Adam C. Pope · Xiaochun Wang

Received: 4 October 2021 / Accepted: 6 May 2022 / Published online: 31 May 2022

Abstract Successful migration of Chinook Salmon (*Oncorhynchus tshawytscha*) smolts seaward in the Sacramento – San Joaquin River Delta (hereafter, Delta) requires navigating a network of numerous branching channels. Within the Delta, several key junctions route smolts either towards more direct paths to the ocean or towards the interior Delta, an area associated with decreased survival. Movements within these junctions that determine route choice can be influenced by numerous behavioral and environmental factors, including the complex interplay between tidal and riverine hydraulics. Here, we apply continuous time multistate Markov models to examine the influence of tidal and riverine hydraulics, behavioral factors, and management actions on smolt movements. These models incorporate more information from acoustic telemetry data compared with previous approaches to modeling smolt movements in the Delta. By decomposing modeled flows into tidal and net flow signals we elucidate how each component influences movements into and out of distributary channels. Increasing net flows generally increased movement rates, while flood tides decreased seaward movement rates. Similarly, ebb tides increased downstream movements as fish go with the flow. We found less support for diel movement behaviors compared to flow metrics. Additionally, we quantify the effects of a large management action, the placement of a physical barrier, which was effective at decreasing entrainment into the interior Delta. Together, these results help inform management of Chinook Salmon and increase our understanding of the major factors driving smolt movements within these key junctions.

Keywords Migration · Multistate models · Acoustic telemetry · Chinook Salmon · Barriers

Supplementary Information The online version contains supplementary material available at https://doi.org/10.1007/s10641-022-01273-1.

M. J. Dodrill (✉) · R. W. Perry · A. C. Pope
Western Fisheries Research Center, US Geological Survey, 5501A Cook-Underwood Road, Cook, WA 98605, USA
e-mail: mdodrill@usgs.gov

X. Wang
California Department of Water Resources, Bay – Delta Office, Sacramento, CA 95819, USA

Introduction

Migration is a widespread behavior in fishes and is an essential component of many life histories (Lennox et al. 2019). For many salmonid species, successful navigation of migration routes, both as smolts actively moving seaward and as adults returning to natal streams, is essential to reproduction and continued population success. Human alterations to riverine systems are widespread and have complicated migration for salmon, often making it more difficult to complete (National Research Council 1996). Although considerable improvements have been made, removing or diminishing barriers to successful migrations (Johnson and Dauble 2006; Evans et al. 2008; Adams et al. 2014), there still exists a large need for evaluation and mitigation of human impacts to migrating species, especially imperiled runs of salmon. Complete migrations often occur across broad spatial scales, yet acute human impacts to migrating fish often occur at much smaller scales, where local conditions and finer scale movements are important to defining ultimate migration success. Understanding factors that influence movements at these key points along migration routes will help provide more robust management of species and facilitate recovery of species of concern.

The Sacramento – San Joaquin River Delta (hereafter, Delta) in California, USA is a complex network of channels that has been highly altered to direct water towards pumping stations in the interior Delta (Nichols et al. 1986). Salmonids, including threatened populations of Chinook Salmon (*Oncorhynchus tshawytscha*) originating from the San Joaquin River, must successfully navigate these channels when emigrating as smolts. Fish that migrate through the interior Delta face many challenges and Chinook Salmon originating from the Sacramento River basin have lower survival likely due to the combined influence of higher predation rates, longer migration times, and entrainment into water pumping stations (Newman and Brandes 2010; Perry et al. 2013). Similarly, steelhead (*Oncorhynchus mykiss*) smolts migrating from the San Joaquin River basin may experience decreased survival traversing sections of the interior Delta (Buchanan et al. 2021). However, Buchanan et al. (2018) found no evidence for lowered survival of acoustic-tagged fall-run Chinook Salmon that entered the interior Delta. Despite the uncertainty related to smolt survival, managers would often like to understand and potentially influence which migration routes are utilized by migrating salmonids: for instance, routing fish towards more direct paths to the ocean or away from water infrastructure, such as pumping facilities. Understanding the driving factors that influence which migration routes are utilized by Chinook Salmon smolts would benefit conservation and recovery of threatened populations in the Delta.

Salmonid smolts migrating seaward from the Sacramento and San Joaquin rivers encounter several key junctions that route fish either towards the interior Delta or towards more direct routes to the ocean. These key locations have received considerable management attention directed at understanding factors that affect fish routing and evaluation of barriers and guidance structures (Perry et al. 2014; Plumb et al. 2016; Romine et al. 2016). Hydraulic conditions such as tidal forcing or water velocity can influence routing of juvenile salmonids at these junctions (Steel et al. 2013; Perry et al. 2015). These hydraulic conditions may interact with fish behaviors such that the timing of arrival at a junction due to nocturnal migration behavior can also influence routing (Chapman et al. 2013; Plumb et al. 2016). Most of the investigations of routing in the Delta have focused on the Sacramento River and northern region of the Delta (references, above), with much less focus on smolts originating from the San Joaquin River. Untangling the influence of competing environmental, behavioral, and management effects that influence routing remains challenging for researchers and managers seeking to better understand these effects.

To date, most studies of smolt routing in the Delta have not utilized the full potential of the rich acoustic telemetry data that is often collected to characterize fish movement. Up until now, most analyses of routing condense movement at a given junction into a single routing event and assign covariates (e.g., various flow metrics) for each routing event using the metrics at the time of entry to the route or junction (Perry et al. 2015; Plumb et al. 2016; Romine et al. 2016). However, in tidally forced estuaries, hydraulic conditions that affect routing may vary on hourly timescales during the time fish are actively transiting a junction. Moreover, the flow may fully reverse during flood tides, causing fish to traverse a junction numerous times before being entrained into a final channel. Under these circumstances, standard approaches like logistic regression cannot fully account for the effect of varying conditions or multiple routing events for an individual fish.

Dynamic hydraulic conditions, environmental or behavioral cues, and management actions interact in potentially complex ways to influence migration routes chosen by Chinook Salmon smolts in the Delta. Understanding the importance of these various factors represents a challenge for managers seeking to balance multiple objectives such as supporting conservation and recovery efforts of salmon and meeting other resource and water management goals. Here, we apply a continuous-time multistate model to quantify the effects of management actions and environmental conditions on routing of juvenile salmon at critical junctions in the Delta. The modelling approach we utilize incorporates high resolution environmental data and accounts for multiple routing events, incorporating the full history of detections and conditions experienced as juvenile Chinook Salmon navigate junctions.

Methods

Study area

The Delta is the largest estuary on the west coast of North America, formed by the confluence of the Sacramento and San Joaquin rivers, along with an array of smaller river systems. Occupying the uppermost portions of the San Francisco Estuary, this region is important for California's water supply, as nearly 50% of the surface water runoff from California passes through the Delta (Nichols et al. 1986). This water supports 25 million people who depend on it for municipal and agricultural use and supports a multibillion dollar agricultural economy (Brown and Bauer 2010).

The Delta consists of a network of branching channels, spanning a gradient of riverine and tidal influences, creating a dynamic environment for juvenile salmonids to navigate. Two major river systems converge in this region, the San Joaquin River that flows northwesterly and the Sacramento River that flows southward (Fig. 1). Salmonid smolts migrating northwestward down the San Joaquin River pass by multiple junctions with distributaries on their migration seaward. Here, we modeled smolt movements at two important junctions, head of Old River (HOR) and Turner Cut (TC, see Fig. 1). These locations are important for juvenile Chinook Salmon migrating in the San Joaquin River because both junctions will route fish either towards the interior Delta or along the mainstem San Joaquin River.

Telemetry data

For all analyses, we used telemetry data from hatchery-reared, fall-run Chinook Salmon implanted with microacoustic transmitters and released into the San Joaquin River at either Durham Ferry, Medford Island, or Stockton. For HOR, we modeled fish released in 6 years, 2011 through 2016, and for TC, we modeled fish released in 2 years, 2015 and 2016. Fish released at Durham Ferry were used in the HOR analysis. For TC, we used fish released at all three release locations, however the majority of fish (89%) used in the analysis were released at Stockton (see Fig. 1). These fish were reared at Merced River Fish Hatchery in 2011 through 2013 and at Mokelumne River Fish Hatchery in 2014 through 2016. In 2011, fish were tagged with Hydroacoustic Technology, Inc. (HTI) Model 795 microacoustic tags. In 2012 through 2016, Vemco V5-180 kHz tags were used. For additional fish tagging and telemetry details see Buchanan and Skalski (2020).

Tagged salmon were monitored using fixed-site acoustic receivers ("telemetry stations"). At HOR, three fixed telemetry stations provided data, with each station consisting of multiple receivers located upstream of the junction and downstream in both the Old River and the San Joaquin River (see Fig. 1). Similarly, at TC, three fixed telemetry stations composed of multiple receivers and located upstream and downstream of the junction in the San Joaquin River and in Turner Cut were used.

We used a subset of the total smolts released, only modelling fish that were detected entering the junction (at any telemetry station) and were subsequently detected at another telemetry station comprising the junction. This allows for detections on the same telemetry station, given fish also were detected at another station in the junction. The telemetry data we model consisted of 2,921 and 369 acoustic-tagged smolts that entered the HOR and TC junctions, respectively. Fish generally transited junctions during April and May. We characterized the time spent in each junction by calculating a sojourn time, defined as the elapsed time from when a fish first enters a junction to the final detection at the junction. Sojourn times were generally short (with median times ranging from 1 to 11.2 h, see Figs. S1 and S2 for summary statistics) and we used the maximum sojourn time as an upper bound for the time-period considered while modelling (see below).

The acoustic telemetry data that we model were processed from the raw detection data to "visit" level data following the methods described in Buchanan et al. (2018). This involves several processing steps done by the U.S. Geological Survey in Sacramento, California and the University of

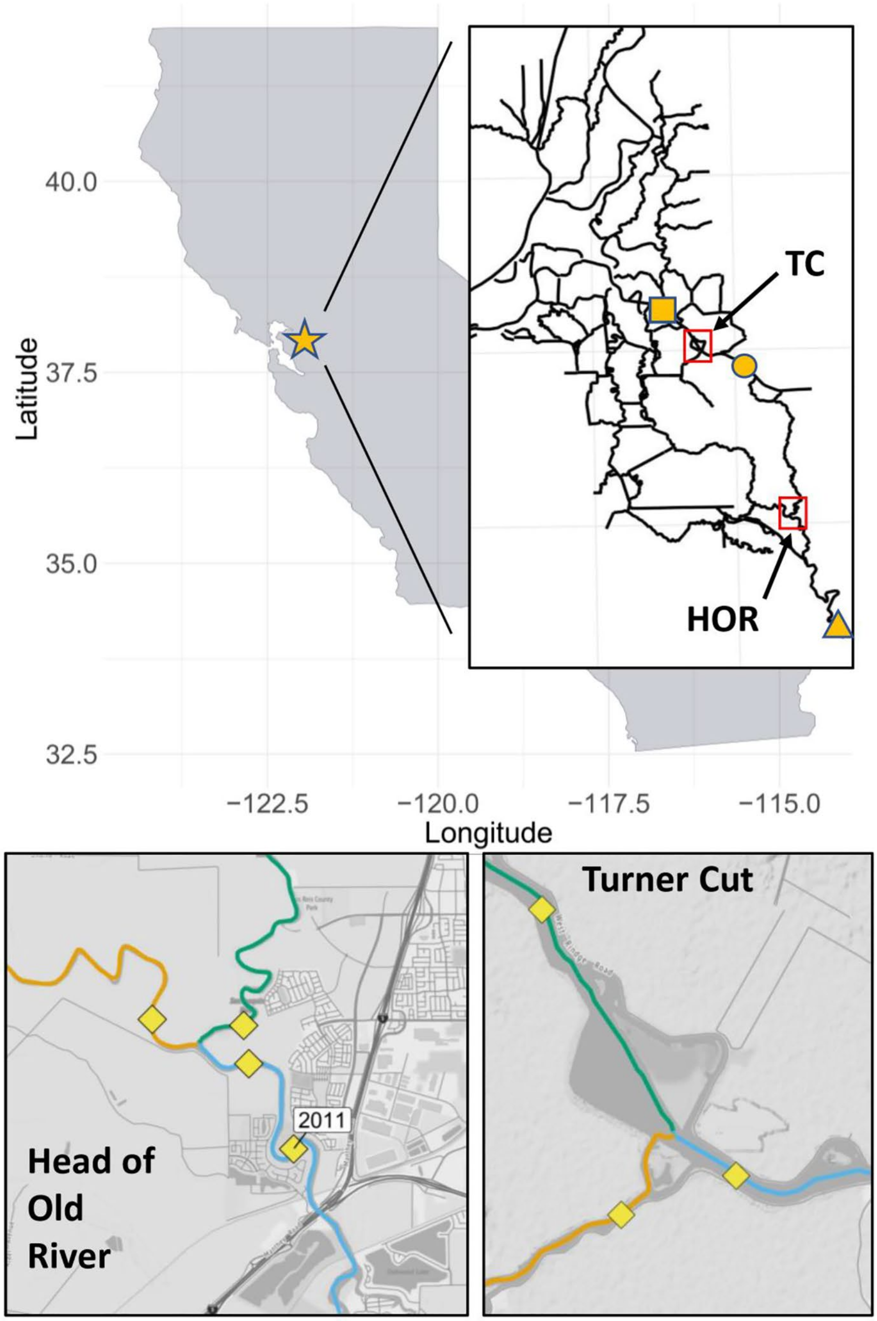

Fig. 1 Map of the study area showing the two junctions of interest: head of Old River (HOR) and Turner Cut (TC). The top inset shows the location of both junctions within the Sacramento—San Joaquin River Delta and the location of the Delta in the state of California, USA. The bottom two insets show each of the junctions in detail, with the upstream San Joaquin River state shown in light blue, the downstream San Joaquin River state shown in green and the distributary (either Old River or Turner Cut) shown in orange. The location of the telemetry stations are shown as yellow diamonds at each junction. Note the location of the upstream telemetry array at HOR in 2011. The release locations are indicated by a triangle (Durham Ferry), a square (Medford Island), and circle (Stockton)

Washington, Seattle. A filter was applied to screen telemetry data for predators that may have consumed the tags and only those identified as smolts were used in the analysis. We used the full filtering process described in Buchanan et al. (2013) and refer readers to more information available in Buchanan et al. (2016).

Data analysis

Routing at junctions entering the Delta from both the Sacramento and San Joaquin rivers has been examined using a variety of approaches, from logistic regression (Cavallo et al. 2015) to integrated Bayesian models (Hance et al. 2020). Our approach differed from prior studies by incorporating the full time series of detections at junctions, instead of summarizing these detections into only the eventual route utilized by fish. A characteristic of the observed telemetry data is frequent detections of fish moving among channels in each distributary junction as fish interact with riverine and tidal forces (Fig. 2, Panel a). When collapsing detections into the final route utilized by fish, associated covariates must also be summarized to match the simplified detection data. This process discards potentially important information by ignoring the time series of environmental conditions over the time period during which fish are moving between detection stations within a junction. In contrast, we employed multistate time-to-event models, which have the advantage of utilizing the full time series of continuous covariates during the time period over which an individual fish transited a junction. This modeling framework is attractive for our application given the complex flow and tidal dynamics fish experience at junctions within the Delta (Fig. 2, Panel b and c).

Although some multistate mark-recapture models also contain routing or transition probabilities (between states representing different routes, Perry et al. (2018)) the methodology described below differs substantially from these types of models. Only parameters representing movements between states

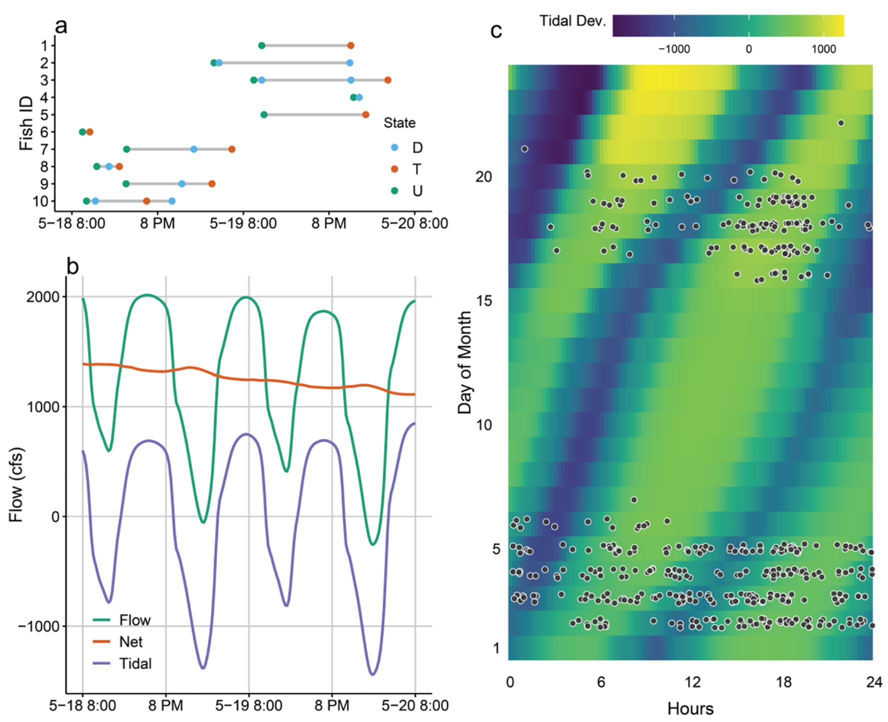

Fig. 2 Figures illustrating elements of both the smolt telemetry data and aspects of the continuous flow covariates in the Sacramento – San Joaquin River Delta, California, USA, in May 2013. Panel a shows a series of detections (points) at the head of Old River junction in different states (colors, see Fig. 3 for state definitions) for 10 individual smolts. These smolts were chosen to represent the frequent transitions between multiple states observed in the data. Points represent the observed time when fish enter a state at the start of each detection event. Panel b shows the 15-minute simulated DSM2 flow (Flow), as well as the filtered riverine (Net) and the tidal (Tidal) components of flow across 48 h during May 18th and 19th, 2013. The data represented in Panel b are from the upstream San Joaquin River location (U) at the head of Old River junction and were chosen to illustrate the sub-daily variation in the tidal component as well as the declining net flow signal (riverine component). Panel c is a heatmap of tidal deviations at the upstream San Joaquin River location (U) over a 24 day period in May of 2013. Hours in the day are shown along the x-axis, while days of the month are shown along the y-axis. Circles represent times that smolts entered the head of Old River Junction (n = 457, all smolts analyzed in 2013). This time period demonstrates the dynamic nature of flow conditions at junctions in the Delta and shows how the tidal deviations progress across a longer time period

are estimated based on observed transitions between telemetry stations. Hence, no detection process is modelled. The implicit assumption is that detection probability does not vary in a systematic way between telemetry stations. Buchanan and Skalski (2020) analyzed these same telemetry data in the context of capture-recapture and found detection probability to be very high, often ≥ 0.98. Also, due to the short time frames during which smolts transit junctions (generally hours, see sojourn times Figs. S1 and S2), and processing of the data (applying the predator filter and only considering observed movements), no survival process is considered (i.e., no mortality occurs).

We used continuous-time multistate Markov models (Jackson 2011) to estimate transition rates of fish between 3 "states" at routing junctions. In our application, each "state" constitutes the three telemetry arrays that bounded each junction. Tagged fish detected at telemetry arrays upstream of the river junction were assigned to an upstream state (state U, Fig. 3). Fish could transition to either downstream state at junctions representing either the downstream San Joaquin River (state D) or downstream distributary (either Old River or Turner Cut, state T). Additionally, we allowed transitions between all states to account for movements between telemetry arrays, a feature of the data that was commonly observed as fish interact with river flow and tidal forces. For example, Fig. 2 Panel a shows 10 individual fish records; fish ID 10 is observed entering the junction in state U, then moving to state D and then state T, before finally moving to state D. Once fish enter a state, they are assigned to this state at intervening times when covariates are observed until they transition to a different state. State entry is defined by the first detection event at a telemetry station bounding the junction and fish switch states at the first detection event at an alternate telemetry station.

Individuals entering either seaward state (D or T) at each junction as their final observed state transition were assumed to continue seaward. This assumption is based on the study fish representing actively migrating smolts. However, no states were absorbing; that is, every state was allowed to have a non-zero probability of transitioning to another state.

Individual fish transition from state $r(t)$ at time t to state $s(t+dt)$ at time $t+dt$ at a rate of $q_{rs}(t)$. The transition rate matrix $Q(t)$ with elements $q_{rs}(t)$ represents the instantaneous transition rate from state r to state s. In our model, the times between state transitions are assumed to be distributed as exponential random variables with rate q_{rs} and mean time to transition $1/q_{rs}$. Our goal was to quantify how time-varying hydrodynamic conditions affected these state transition rates. The data for fitting this model are organized into a 15-minute time series of occupied states for each individual, where S is the set of possible states $S \in (\mathrm{U,D,T})$, $S(t=0)$, $S(t=1)$, …, $S(t=T)$ for $t=0, 1, \ldots, T$ times after the first detection at a telemetry array until an upper limit for the time period of interest is reached. We define this upper limit of time modelled as 5.5 days, given the maximum observed

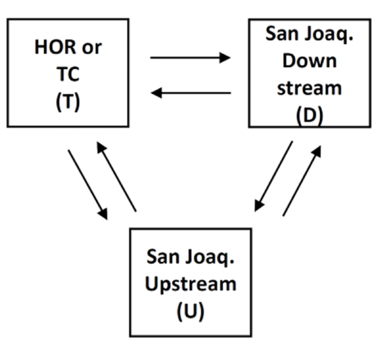

$$Q = \begin{array}{c} \\ U \\ D \\ T \end{array} \begin{array}{c} \begin{array}{ccc} U & D & T \end{array} \\ \begin{bmatrix} -(q_{UD}+q_{UT}) & q_{UD} & q_{UT} \\ q_{DU} & -(q_{DU}+q_{DT}) & q_{DT} \\ q_{TU} & q_{TD} & -(q_{TU}+q_{TD}) \end{bmatrix} \end{array}$$

HOR

$$\begin{bmatrix} 49 & 1928 & 971 \\ 36 & 70 & 27 \\ 8 & 1 & 12 \end{bmatrix}$$

TC

$$\begin{bmatrix} 25 & 381 & 21 \\ 96 & 53 & 16 \\ 4 & 1 & 2 \end{bmatrix}$$

Fig. 3 Schematic of the multistate model and state transition matrix used to estimate transition rates (q_{rs}) of Chinook Salmon smolts. States are defined as San Joaquin Upstream (U), San Joaquin Downstream (D), and head of Old River or Turner Cut (T). The lower two matrices show the observed number of state transitions for HOR and TC, respectively. For state transition matrices, starting states are listed as rows ("from") and finishing states are listed as columns ("to"). For example, at HOR, 1928 transitions were observed from state U to state D sojourn time of 5.4 days, so that all observed movements have occurred during this time period. These multistate time to event models can accommodate multiple observation types. We include two types of observations. First, the exact transition times are used when fish are first detected at telemetry stations. The majority of these observations occur as fish move and are detected at different stations within a junction. However, a smaller number occur after a period of time at the same station when a fish is detected during a new detection event (for instance U-U, see Fig. 3). Second, the intervening 15-minute time series are treated as panel-observed data where observations occur at arbitrary times (here, our 15-minute time interval). Panel observed data are common in medical applications where subjects (here, fish) are followed over time and observations of states, such as disease status, are recorded at a regular frequency (such as at monthly or annual exams, here our 15-minute time interval). Because state transitions (movements) are modeled in continuous time, these two types of observations (e.g., at exact transition 01:28:32, or the following 15-minute interval, 01:30:00) can be easily combined. Importantly, the state in panel data does not denote the precise time of transition to that state, only that the individual was in a particular state at the time of observation. For example, the disease status noted in an annual exam could have arisen at any time between that exam and the previous observation for that individual. Panel observed data represent only a snapshot in time of a given state, and transitions among states in the intervals between these observations are allowed in the model.

The modelling approach allowed for the inclusion of covariates affecting transition rates. We expressed transition rates as a log-linear function of covariates;

$$q_{rs}\left[z_i(t)\right] = \exp\left(\beta_{rs,0}\right)\exp\left[\beta_{rs}^T z_i\left(t\right)\right]$$

where $z_i(t)$ is a vector of covariates for individual i at time t; $\exp(\beta_{rs,0})$ is the baseline hazard rate; β_{rs} is a vector of slope coefficients; and $\exp(\beta_{rs,k})$ is the hazard ratio for the kth covariate. We fit models to data using the "msm" package (Jackson 2011) in R version 4.0.5 (R Core Team 2021). The model fitting used maximum likelihood to estimate model parameters and standard errors. We assessed the significance of model coefficients by whether the 95% confidence intervals overlapped a value of one.

Covariates

We used the Delta Simulation Model II hydrodynamic model (DSM2 HYDRO) to generate 15-minute flow data. The DSM2 model is a one-dimensional hydrodynamic model that simulates flows, velocities, depth, and water surface elevations in the Delta's network of channels. The model has been extensively developed, tested, calibrated periodically, and used by the California Department of Water Resources (CDWR) and other state and federal agencies for planning water resources management related projects. We used DSM2 simulations that represented conditions during periods when tagged fish migrated through the Delta. At each of the telemetry stations bounding the junctions, we generated a time series of flows to use as covariates (Figs. 4, S3, S4, S5). At TC we applied a 90-minute lag to the simulated DSM2 flows to correct for a phase shift in the tidal signal between observed and simulated flows, as identified in the 2009 CDWR calibration report (CDWR 2009).

To decompose riverine from tidal flow, we applied a Godin filter (Godin 1972), resulting in filtered flows that we term "net flow" (Net) and tidal deviations (Tide). The net flow represented the riverine component of flow while the tidal deviations represented the tidal component. This decomposition of flows into tidal and riverine components was done for each telemetry station. Additionally, we categorized flows into a binary variable (Rev), representing any reversal of flow in each channel. We coded this variable as $Rev = 0$ to represent seaward flow and $Rev = 1$ to represent upstream or inland flow. Note that the positive direction of net flow in Turner Cut is towards the mainstem San Joaquin River, and thus the indicator for reversal of flow will be switched relative to other channels in the junction. We used the time-series of continuous covariates at the receiving state to represent these covariate effects on movements. For instance, for modeling of q_{UD} the time-series of covariates from the downstream San Joaquin River telemetry stations were used. Similarly, for modeling q_{UT}, covariates from either HOR or TC were used.

Management agencies have installed various temporary physical or nonphysical barriers at the head of Old River since the 1990s. A temporary rock barrier was installed in 2012 and 2014–2016 near the head of Old River that included culverts that allowed for limited water and fish passage. We included the

Fig. 4 Time series of flows (orange) and net flows (green) in the San Joaquin River at the upstream telemetry station bounding the Old River junction. Each panel represents the flow conditions over the range of time when smolts were transiting the junction each year. See Figs. S3, S4, and S5 for plots of tidal deviations and flow covariates at Turner Cut

barrier status in our model as a binary variable (Bar) representing conditions where the barrier was either present ($Bar = 0$) or absent ($Bar = 1$). The barrier was considered present after the date each year when installation was fully complete and absent after the date when the barrier was first breached during removal. The effect of the barrier was assessed by adding terms for barrier status that affect the possible movements to Old River and the downstream San Joaquin River telemetry station. Note that the barrier was absent in 2011, a year with elevated flows in the San Joaquin River in contrast to lower flows that occurred in 2013.

Prior studies of migrating smolts have identified nocturnal migration behavior (Chapman et al. 2013). We considered nocturnal migration behavior of smolts by including a binary variable (Day) representing either night ($Day = 0$) or day ($Day = 1$), mutually exclusive categories. Day and night were defined based on daily times of sunrise (top edge of the sun appear on the horizon) and sunset (sun disappears below the horizon), generated using the R package 'suncalc' (Thieurmel and Elmarhraoui 2019), for the latitude and longitude of either HOR or TC.

Due to the limited sample size for some state transitions and our focus on upstream to downstream movements, we only included covariate effects on q_{UD} and q_{UT} for HOR (Fig. 3). For TC, we modeled covariate effects on q_{UD}, q_{UT}, and q_{DU}. The choice to limit the model complexity considered here (i.e., not include covariates on all transitions) is a practical one given the limited observations of some transitions in the dataset (see Fig. 3). This does not assume that these transitions are not likely influenced by hydrologic (or other) factors, rather, that given the current data, we are unlikely to statistically fit or meaningfully interpret these relationships. For transitions which included covariate effects, we assumed the same covariate structure for all state transitions when fitting each model. Further, we did not consider models where movements varied by year.

We fit 19 and 16 alternative models for HOR and TC, respectively. For both junctions, the simplest model assumed that all transition rates were constant. Generally, the telemetry stations were in similar locations across years with the exception of the upstream station at HOR in 2011, when it was located approximately 2.36 km further upstream (see Fig. 1). For HOR, our model selection approach proceeded in two steps. First, we included the barrier and a 2011 effect (2011, representing the change in the telemetry station location), both singularly and together and compared these models with a no covariate model. Next, we chose the most highly supported model and kept this structure constant while fitting more complex models including the flow and behavioral effects. For TC, the model set was smaller due to no barrier or 2011 effect, and we fit models including flow and behavioral effects. At both locations, we did not consider models that contained both the flow effect and the decomposed flow (tidal and net flow signals), as all the information contained in the flow effect is duplicated by these other terms. Further, we did not consider the reversing flow and tidal terms in the same model but included these alone or with other factors. We then used Akaike's information criterion (AIC) to select the most parsimonious model at each location for inference (Burnham and Anderson 1998).

Given the most highly supported model for each junction, we examined the covariate effects on transition rates by (1) summarizing the estimated slope coefficients, (2) plotting the effect of covariates on the probability of state transition (for HOR), and (3) plotting the n-step transition probabilities over a 72-hour time series of covariates (for TC). The probability of transitioning from state r at time t to state s after one 15-minute timestep is

$$P(t+1|z(t)) = Exp(Q(z(t)))$$

where $P(t+1|z(t))$ is the transition probability matrix conditional on covariates $z(t)$ at time t and where 'Exp' represents the matrix exponential function. The transition rate matrix is denoted by $Q(z(t))$ with elements q_{rs} and depends on covariates $z(t)$.

We used n-step transition probabilities (Lindsey 2004) to illustrate the effects of a time series of covariates on movements and to provide insights into the expected final fate of fish:

$$P_n(t+n|z(t),\ldots,z(t+n-1)) = \prod_{t=1}^{n} P(t+1|z(t))$$

where P_n is the n-step transition matrix whose elements represent the probability of transitioning from state r at time t to state s after $t+n$ timesteps, given the entire set of covariates between time t and $t+n$-1. Here, the product symbol indicates matrix multiplication. Furthermore, as n increases, n-step transition probabilities that approach a quasi-equilibrium (i.e., remain relatively stable with time) and are analogous to the stable stationary state distribution of a time-constant Markov chain where the proportion of individuals in each state is constant through time (Lindsey 2004). That is, stable n-step transition probabilities approximate the final expected proportion of individuals in each state. In our application, the n-step transition probabilities provide insight into how a given time series of covariates affects the final fate of fish in terms of the expected long-run probability of entering a given channel.

In our application, because state transition probabilities represent movements between telemetry stations, hereafter we refer to transition probabilities as movement probabilities. Lastly, we compared the expected and observed prevalences (the number of individuals occupying each state, represented as percentages) at a series of discrete times, starting at the initial time of entering each junction. This comparison is typically used to assess goodness of fit of multistate time to event models and we included plots of the observed and predicted proportions across 72 h (see Supplementary Information).

Results

The majority of smolts transited junctions in a short period of time. At HOR, the median sojourn times ranged from 1 h to 2012 to 4.2 h in 2015 (Fig. S1). At TC, smolts transited in a median time of 6.2 and 11.2 h in 2015 and 2016, respectively (Fig. S2). At HOR, once fish entered the junction, the majority moved downstream in the San Joaquin River with 1,928 observations representing 62% of all observed transitions, followed by movements into Old River (971 observations, 31%, see Fig. 3). Relative to upstream-to-downstream movements in the San Joaquin River, upstream movements or changing of routes were less frequent, representing 1–2% of observations. At TC, upstream to downstream San Joaquin River movements again represented most observations (64%), while movements into Turner Cut represented considerably fewer (~4%). Likely due to the larger tidal influence at TC, upstream movements and route switching were more common. For example, 16% of the observed movements were from downstream to upstream in the San Joaquin River.

To describe routing at HOR, we fit 19 competing models in a two-step process. First, we considered the effect of the telemetry array placement in 2011 and barrier status. Both effects were retained and then carried forward in all subsequent model fitting and appear in the most highly supported model (Table 1). The most highly supported model included the decomposed effects of both tides and net flows. In addition, this model included the behavioral effect of movements rates differing during the day versus night. The top model was separated from the next most highly supported model by 9.0 ΔAIC. The second most highly supported model only differed by the exclusion of the behavioral day versus night effect. All other HOR models were separated by greater than 10 ΔAIC. Models including the term representing flow (both riverine and tidal signals combined) did not receive support.

Table 1 Model selection table comparing competing models of routing at head of Old River (HOR) and Turner Cut (TC)

Location	Model	k	AIC	ΔAIC
HOR	2011 + Bar + Net + Tide + Day	16	25226.2	0.0
HOR	2011 + Bar + Net + Tide	14	25235.2	9.0
HOR	2011 + Bar + Flow + Day + Rev	16	25241.0	14.8
HOR	2011 + Bar + Flow + Day	14	25243.2	17.0
HOR	2011 + Bar + Flow + Rev	14	25251.4	25.3
HOR	2011 + Bar + Flow	12	25254.3	28.1
HOR	2011 + Bar + Net + Day + Rev	16	25309.2	83.0
HOR	2011 + Bar + Net + Rev	14	25311.0	84.9
HOR	2011 + Bar + Net + Day	14	25384.5	158.3
HOR	2011 + Bar + Net	12	25385.3	159.1
TC	Net + Tide	12	6007.6	0.0
TC	Net + Tide + Day	15	6011.8	4.2
TC	Flow	9	6060.5	53.0
TC	Flow + Rev	12	6063.0	55.4
TC	Flow + Day	12	6064.9	57.3
TC	Flow + Day + Rev	15	6066.7	59.2
TC	Flow	9	6084.9	77.3
TC	Net + Rev	12	6089.4	81.9
TC	Flow + Day	12	6089.6	82.0
TC	Net + Day + Rev	15	6092.0	84.5

Note, only the top 10 most highly supported models for each location are shown. 2011, offset for year 2011; Bar, barrier status; Net, net flows; Tide, tidal deviations; Flow, discharge; Day, behavioral day versus night effect; Rev, reversing discharge indicator; K, number of parameters; AIC, Akaike's information criterion; ΔAIC, difference between current model and most highly supported model for each location

For Turner Cut, we fit 16 competing models with the most highly supported model containing tidal and net flow effects (Table 1). This model was separated from the next most highly supported model by 4.2 ΔAIC and differed with the inclusion of the day versus night effect. Similar to HOR, all other models were separated by greater than 50 ΔAIC, including models with non-decomposed flow (Flow) effect.

At HOR, net flows had a positive effect on the movement rates from upstream to downstream in the San Joaquin River and into Old River (Fig. 5; Table 2). The net flow effects were significant and strong in comparison to other non-barrier effects,

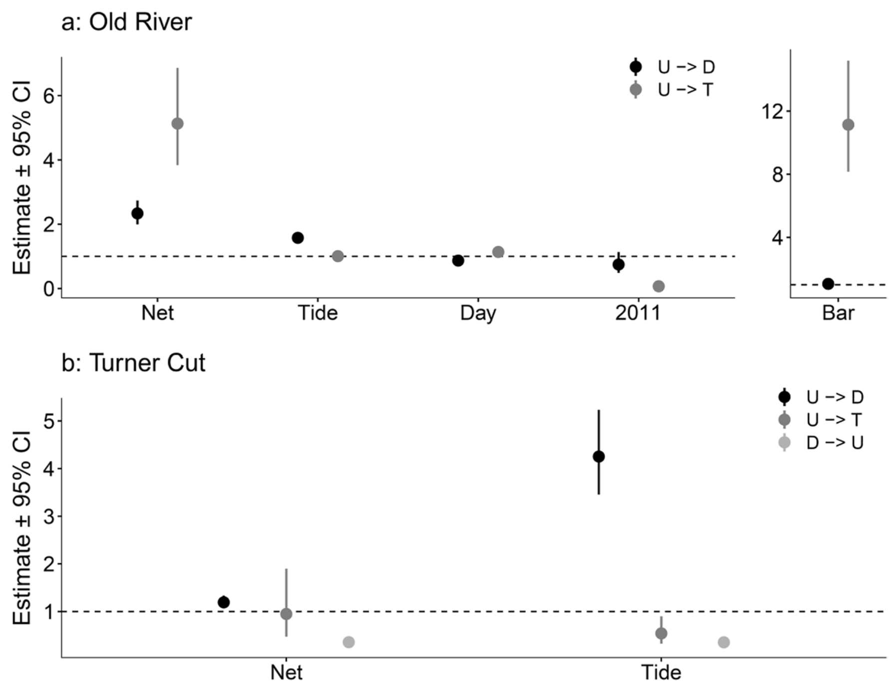

Fig. 5 Coefficient estimates and 95% confidence intervals from the most highly supported model at head of Old River (Panel a) and Turner Cut (Panel b). Note the separate y-axis for the barrier effect. For discrete covariates, Day represents the effect of daytime ($Day = 1$), 2011 represents the year 2011 and Bar represents the effect of the barrier being absent ($Bar = 1$) at the head of Old River. States are defined as San Joaquin Upstream (U), San Joaquin Downstream (D), and head of Old River or Turner Cut (T)

indicating that fish move more quickly from upstream to both seaward states with increasing net flows. The barrier effect on movement from upstream San Joaquin River into Old River was significant and strong, indicating that when the barrier was absent, smolts have a much higher movement rate into Old River. The barrier also decreased movements from the upstream to downstream San Joaquin state when the barrier was absent, as more fish moved into Old River. The most highly supported model for HOR also included terms for tidal effects, with a significant positive effect on upstream to downstream San Joaquin River movement rate, indicating that fish moved more quickly during ebb tides. Conversely, fish moved more slowly from upstream to downstream in the San Joaquin River during flood tides. The 2011 effect was also represented in the top model, indicating that when the telemetry station was located further upstream from the junction, smolts transitioned to seaward states more slowly. Although the most highly supported model included the day versus night effect, this effect was weak compared to other model terms.

At TC, the most highly supported model included terms for both tidal and net flow effects. In contrast to HOR, the tidal effects were generally stronger than the net flow effects. The strongest tidal effect was for the upstream to downstream San Joaquin transition, indicating that seaward movement increased with increasing strength of ebb tides. The opposite transition, from downstream San Joaquin to upstream, had an effect less than one, which can be interpreted as increasing upstream movement rates with flood tides. The tidal term for upstream to TC transitions was less than one, suggesting that ebb tides decreased the transition rate into TC. Although the net flow effects were generally weaker than the tidal components, several of these terms were significant for the San Joaquin River portion of the junction. Increasing net flows increased the upstream to downstream movement in the San Joaquin River and similarly slowed downstream to upstream movements. The net flow effect for transitioning into Turner Cut was not significant and the 95% confidence intervals overlapped one (values overlapping one represent no significant effect in our model). Table 2 provides the baseline transition rate estimates along with 95% confidence intervals for all terms appearing in the most highly supported models for each junction.

To illustrate the largest effects from the most highly supported model at HOR, we plotted 15-minute movement probabilities across the observed range in net flows, with the barrier either absent or present (Fig. 6). For both movements into the downstream

Table 2 Parameter estimates (with 95% confidence intervals in parentheses) from the most highly supported models for both junctions (see Table 1)

Junction	Transition	Term	Estimate
HOR	q_{UD}	Baseline	4.297e-02 (4.083e-02, 4.522e-02)
		Net	**2.335 (1.996, 2.733)**
		Tide	**1.575 (1.460, 1.700)**
		Day	**0.868 (0.792, 0.952)**
		2011	0.746 (0.491, 1.132)
		Bar	1.058 (0.867, 1.293)
	q_{UT}	Baseline	1.566e-02 (1.417e-02, 1.731e-02)
		Net	**5.133 (3.840, 6.862)**
		Tide	1.006 (0.953, 1.062)
		Day	1.136 (0.999, 1.292)
		2011	**0.069 (0.040, 0.120)**
		Bar	**11.136 (8.162, 15.193)**
	q_{DU}	Baseline	5.055e-05 (3.639e-05, 7.021e-05)
	q_{DT}	Baseline	3.731e-05 (2.558e-05, 5.440e-05)
	q_{TU}	Baseline	2.163e-05 (1.081e-05, 4.324e-05)
	q_{TD}	Baseline	4.182e-06 (8.847e-07, 1.977e-05)
TC	q_{UD}	Baseline	5.542e-03 (4.530e-03, 6.779e-03)
		Net	**1.193 (1.066, 1.335)**
		Tide	**4.253 (3.457, 5.232)**
	q_{UT}	Baseline	5.237e-04 (3.115e-04, 8.806e-04)
		Net	0.949 (0.474, 1.900)
		Tide	**0.541 (0.326, 0.898)**
	q_{DU}	Baseline	4.211e-04 (3.061e-04, 5.795e-04)
		Net	**0.357 (0.284, 0.448)**
		Tide	**0.354 (0.275, 0.455)**
	q_{DT}	Baseline	1.378e-04 (8.453e-05, 2.246e-04)
	q_{TU}	Baseline	3.325e-04 (1.249e-04, 8.854e-04)
	q_{TD}	Baseline	7.751e-05 (1.020e-05, 5.885e-04)

Baseline represents the intercept or baseline transition rate for each transition; 2011, offset for year 2011; Bar, barrier absent (*Bar* = 1); Net, net flows; Tide, tidal deviations; Day (*Day* = 1), day versus night effect. Bold values indicate covariates that were significant (i.e., their 95% confidence intervals did not overlap 1). Estimates greater than one for binary variables represent an increase in the transition (movement) rate versus the baseline value as defined and vice-versa. For instance, the barrier effect for $q_{UT}$of 11.3 represents an increased movement rate when that barrier is absent (*Bar* = 1), compared to when it was present (*Bar* = 0). For continuous variables, the estimates represent the slope of the relationship, again with values over one representing a positive effect, increasing the movement rate with increases in the covariate. States are defined as San Joaquin Upstream (U), San Joaquin Downstream (D), and head of Old River or Turner Cut (T)

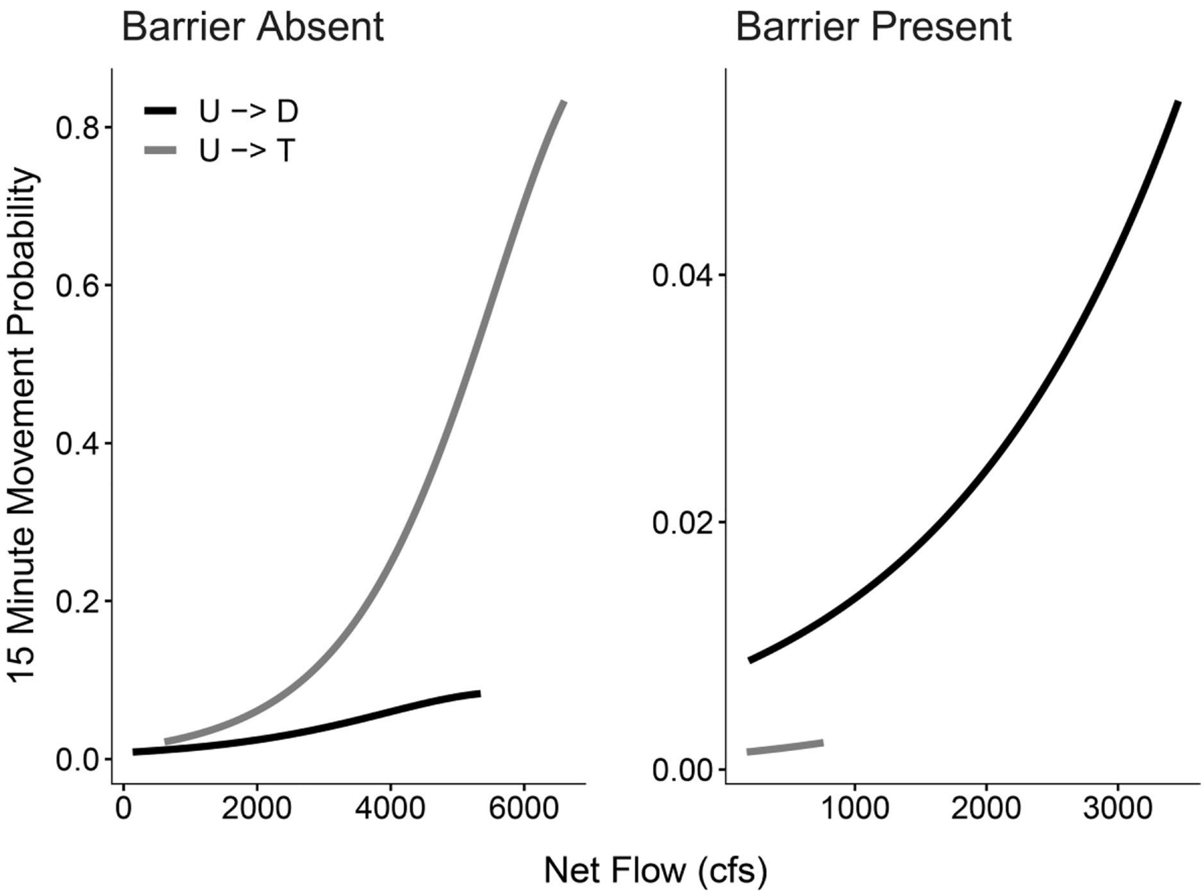

Fig. 6 Effect of net flow (cubic feet per second, cfs) on the 15 min movement probability of Chinook Salmon smolts into either downstream state at the HOR junction with the barrier absent and present. Black and grey represent each of the movements probabilities and these are truncated at the observed range of net flow used in model fitting. For example, movements from state U to state T were observed only across a small range of cfs (177–761) when the barrier was present. Movement probabilities were calculated from coefficients using the most highly supported model for HOR (see Tables 1 and 2), holding tidal deviations constant at their mean. While varying net flows under one condition (i.e., the range for U to D movements, barrier absent) we used the mean relationship from linear regressions to represent the net flows in the other state across this range (i.e., predicted net flows in T at a given level in D). This regression approach was used due to the relationships in flow between each channel and the unrealistic conditions imposed by a traditional approach (i.e., holding net flows at their mean in each channel while varying the range in the channel of interest). Probabilities were calculated for the day (*Day* = 1) and in a non-2011 year. States are defined as San Joaquin Upstream (U), San Joaquin Downstream (D), and head of Old River (T). Note the large difference in the y-axis scales between the two panels

San Joaquin and Old River, 15-minute probabilities increased with net flow. When the barrier was present, movement probabilities into the downstream San Joaquin River were higher than movement probabilities into Old River. When the barrier was absent, movement probabilities into Old River were higher and this increased with increasing net flow, especially with net flows over 3,000 cubic feet per second (cfs).

We estimated movement probabilities between states over 72 h at TC using observed net flows and tidal deviations, covariates identified in the most highly supported model at this junction (Fig. 7). Using April 2016 as an example, the probability of moving from U to D increased in a step-wise fashion, due to the strong influence of tidal forces (compare Panels a and b, Fig. 7). Other movements at this junction also showed the influence of the tides, although to a lesser extent. At TC, net flows had a smaller influence on movement probabilities and generally

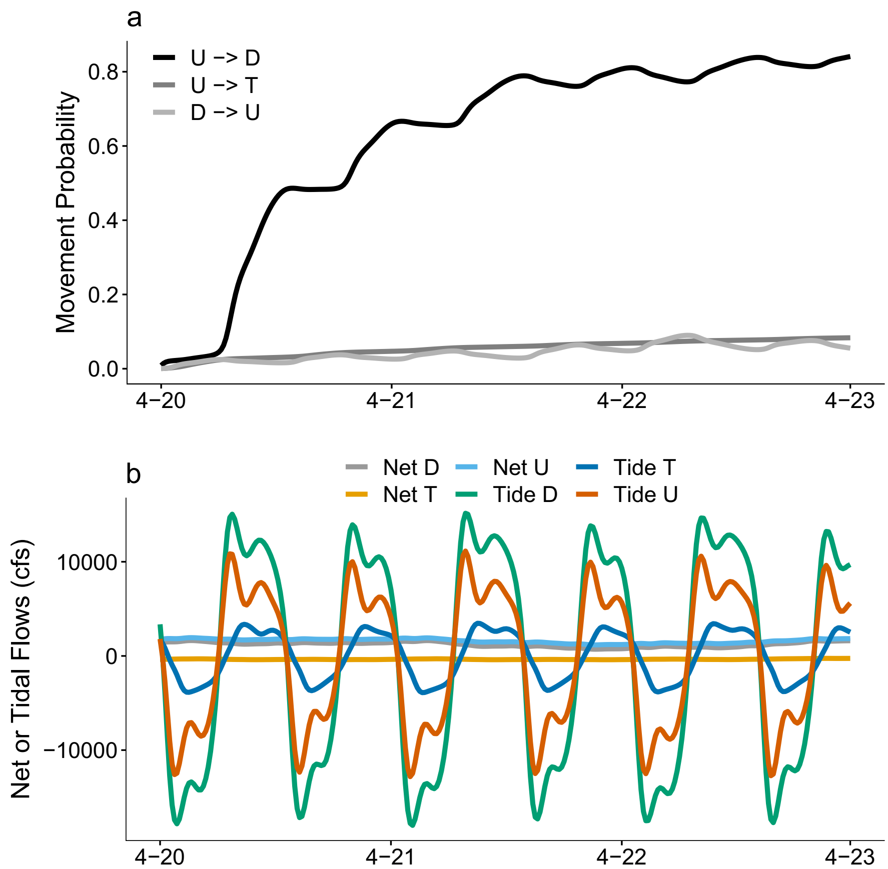

Fig. 7 For the Turner Cut junction, Panel a shows the movement probability between the three states including the covariate effects of tidal deviations and net flows over a 72 h period in April of 2016. The most highly supported model for Turner Cut (see Tables 1 and 2) was used to calculate these movement probabilities. The tidal deviations (Tide) and net flows (Net) used to predict movement probabilities are shown in Panel b, highlighting the dynamic flow conditions which influence routing. Flows are in cubic feet per second (cfs). States are defined as San Joaquin Upstream (U), San Joaquin Downstream (D), and Turner Cut (T)

showed little variation across the time periods used for model fitting.

We did not find any significant lack of fit based on our goodness of fit procedure (Figs. S6, S7). However, the observed data often shows an early and fast transition from state U to states D and T, which our multistate approach often fits as a more gradual transition to these states. Nevertheless, the multistate models performed well when predicting the proportions of smolts that transitioned into each state within 72 h.

Discussion

Our multistate modelling approach allowed for separating the tidal and riverine components of flow, each of which was supported at both junctions and influenced routing of Chinook Salmon smolts. Previous studies of juvenile salmonid routing in the Delta have identified numerous components of net flows as important to routing (Perry et al. 2015; Plumb et al. 2016; Romine et al. 2021). Our results at HOR suggest that net flows have a large influence on routing, with increasing net flows increasing the movement rate into both seaward states. Besides the HOR barrier effect, net flows had the largest influence on smolt movements at this junction. At TC, the effect of net flows was supported by model selection, yet the strength of the net flow effect on transitions was less than at HOR. The lesser effect of net flows at TC could be due to several factors. First, the TC junction is downstream of HOR and generally more tidally influenced. Second, we modeled smolts in TC during only two years, 2015 and 2016, and in these years, during the time periods when smolts transited the junction, net flows exhibited little variation and were generally low due to drought conditions. Applying our modelling approach to additional acoustic telemetry data across the Delta, at locations that represent gradients in riverine and tidal influence, would further elucidate the effects of complex flow dynamics at junctions important to smolt migration. For instance, several locations in the North Delta, such as the Delta Cross Channel, and the entrances to Sutter and Steamboat Sloughs, could be potential areas to apply and test our modelling approach versus previous work (Plumb et al. 2016; Romine et al. 2021).

By decomposing the flows into tidal and riverine components, our methods were able to refine our understanding of how the tides influence smolt movement and routing. Perry et al. (2015) identified the strong influence of tidal forces on Chinook Salmon smolt entrainment at key junctions within the Sacramento River. These authors showed that during reverse-flow flood tides, the entrainment of smolts into Georgiana Slough and the Delta Cross Channel increased and the probability of remaining in the Sacramento River decreased to near zero. Similarly, Romine et al. (2021) found entrainment of smolts into distributaries of the Sacramento River was influenced by the tidal cycle, especially the ascending and descending portions of the cycle where flow changes from positive to negative. Our results demonstrated that movement from upstream to downstream in the San Joaquin River increased with increasing strength of ebb tides. At TC, we observed the downstream to upstream San Joaquin River movement rate decreased with the strength of ebb tides, or conversely increased with the strength of flood tides.

As smolts transit these junctions, they can experience multiple tidal cycles, and we observed switching among routes as fish interact with tidal and riverine flow components. Modelling these transitions within continuous time allows for predictions of how multiple tidal (and net flow) components interact at fine temporal scales to influence routing. For instance, Fig. 7 shows the movement probabilities into multiple states at TC for a 72-hour period, demonstrating how various tidal components interact to shape smolt routing. Note how the movement probabilities approach a quasi-equilibrium, approximating the final long-run probability of entering a channel. While the focus of our application was on identifying fine-scale movements and drivers influencing these movements, this property of reaching stable stationary state distributions provides an additional benefit, estimates of the final proportion of individuals in each channel. Key junctions within the Delta can exhibit complex flow patterns as both tidal and riverine components interact, and the ability to integrate these dynamics at fine temporal resolution improves our understanding of Chinook Salmon smolt routing.

Further understanding how components of flow influence routing at key junctions in the Delta will benefit management of salmonids, especially as river flows change in the coming decades. Freshwater inputs to the numerous rivers that form the Delta may decline and show altered seasonal timing as a result of climate change (Hayhoe et al. 2004; Maurer 2007). If net flows decrease in the San Joaquin River during times of juvenile salmonid passage, fish routing at key junctions will likely be altered. At HOR, our results suggest that net flows have a large influence on fish moving into Old River, which routes fish towards regions of the interior Delta. The implications of routing more juvenile Chinook Salmon smolts from the San Joaquin River into the interior Delta are uncertain. Smolts that enter this region from the Sacramento River often experience lowered survival (Newman and Brandes 2010; Perry et al. 2013). The manner in which future timing and magnitudes of net flows interact with water management decisions will likely determine the routing of Chinook Salmon smolts at HOR. Additionally, if net flows decrease, the role of the tides may increase relative to net flows. Although we only analyzed routing at two junctions, these locations sit along a riverine-tidal gradient and we observed greater influence of tidal forces on routing at TC where the net flows were a minor component of overall flows. Several other seaward junctions (Columbia Cut, mouth of Middle River, and mouth of Old River) also allow smolts to enter the interior Delta and would be excellent locations to explore the influence of tidal forces on fish routing.

Some support exists for diel movement behavior in juvenile salmon within the Delta (Chapman et al. 2013; Plumb et al. 2016). We found some evidence for behavioral effects related to day versus night at HOR, yet this effect was small in comparison to other factors and we did not find support for this effect at TC. Time of day was not supported by model selection in analysis of entrainment of Chinook Salmon by Perry et al. (2015), however these authors found that more fish arrived at telemetry stations during the night compared to during the day. Diel movement behavior can be influenced by numerous factors and behaviors may change in response to trade-offs associated with predation risk, physiological state or various environmental cues (Metcalfe et al. 1998, 1999).

This plasticity in diel movements complicates our understanding of how these behaviors may influence route choice. Overall, our results suggest that diel-related behavioral factors play a minor role in Chinook Salmon routing at HOR and TC compared with net and tidal flow components.

We assessed the influence of the physical barrier at HOR and found a large effect on movements from the upstream San Joaquin River into Old River. When the barrier was absent, smolts had a higher probability of moving into Old River, especially with higher net flows in Old River. For the smolt movement data we analyzed, 2011 had the highest net flows into Old River and represents a year when the barrier was absent due to these high flows. For the range of net flows observed in Old River this year (5250–6602 cfs) smolts had a 0.51–0.83 predicted 15-minute probability of entering Old River. In lower water years, for instance 2013 when the barrier was also absent, the range of net flows (611–2425 cfs) equated to a 0.02–0.08 range in 15-minute probability of entering Old River. Previous analysis of Chinook Salmon smolt entrainment into Old River has estimated the proportions to range from 0.36 to 0.59 (Buchanan et al. 2013). However, the estimates from Buchanan et al. (2013) are based on mark-recapture modelling and refer to the final fate of smolts traversing this junction at larger spatiotemporal scales and do not directly relate to our fine scale 15-minute probabilities. Overall, our results confirm that a physical barrier at HOR has a large effect on routing and that net flows in Old River also influences the probability of fish entering Old River.

Our continuous-time multistate Markov modelling approach utilizes the full time series of continuous covariates when estimating transitions between states, which may offer some distinct advantages versus previous approaches used in the Delta. Logistic regression has often been used to explore routing in the Delta (Steel et al. 2013; Cavallo et al. 2015; Plumb et al. 2016) and while these approaches often perform well at predicting the overall proportion of fish in a route, they often must collapse or discard covariate information useful in explaining routing, especially at sub-daily time scales. For instance, using logistic regressions Cavallo et al. (2015) computed mean daily proportion of flow entering distributaries and related these covariates to routing probabilities. In strongly tidally influenced junctions, where a complete tidal cycle is present within a day, using the daily mean results in a low or near zero covariate value for the tidal flow component (daily negative flows are balanced by daily positive flows), even when strong tidal effects may be present and changing throughout the day. Therefore, continuous-time multistate methods applied at fine temporal scales (e.g., 15-minute, hourly, etc.) have an advantage in estimating tidal or other subdaily time-dependent variables compared to typical methods used to assess routing.

Our results and model application to Chinook Salmon smolts improves our understanding of factors that influence routing at key junctions in the Delta. Much like previous applications of routing models (Cavallo et al. 2015; Plumb et al. 2016; Romine et al. 2021) our approach does not explicitly account for smolt survival nor detection probability. If the implications of route choice in terms of survival are of interest, other modelling approaches, such as multistate mark-recapture models (Perry et al. 2018; Buchanan and Skalski 2020) would be more appropriate. Our approach assumes that detection probability does not vary in a systematic way between arrays. Buchanan and Skalski (2020) analyzed these same telemetry data in the context of capture-recapture and found detection probability to be very high, often ≥ 0.98. Given the high detection probability, it is unlikely that heterogeneity in detection probability would bias the estimated movement probabilities or relationships to covariates in any significant manner. We suggest that authors assess detection probability and survival over time scales relevant to a particular application, as a loss of precision or bias in parameter estimation may results as these probabilities depart from one or vary in a systematic manner. While the approach we present advances several aspects of modelling smolt routing, particularly with understanding the influence of covariates at fine temporal scales, other approaches would be more appropriate to inform population level consequences of these movements and behaviors. Additionally, our modelling relied on acoustic telemetry data which had been processed (following Buchanan et al. (2018)) and a predator filter applied to ensure the modelling of smolts and not predators which had consumed tags. In general, more assessment of the sensitivity of model results to processing of acoustic telemetry data, not only in our application but more broadly, seems warranted.

Many proposed management actions consider alterations to river flows within the complex network of channels in the Delta. The model we present here shows how river flow alteration could influence Chinook Salmon smolt routing. Integrating our statistical methodology with existing hydrodynamics models, such as DSM2, would allow managers to assess the impacts of alternative flow management on flow conditions at key junctions and the predicted smolt movements given a set of flow conditions. The ability to link hydrodynamic simulation models to statistical models of smolt movements at the fine temporal resolution necessary to realistically capture ecological dynamics would provide critical information to inform management of threatened species in the Delta.

Acknowledgements This work was funded by California Department of Water Resources. We extend special thanks to Ryan Reeves and William McLaughlin for their support. We thank Summer Burdick, Rebecca Buchanan, Bryan Matthias and anonymous reviewers. Further, we thank the many people and agencies who oversaw and implemented fish tagging, care, and release, and acoustic receiver installation, maintenance, retrieval, and processing. The data analyzed during the current study are available from the corresponding author on reasonable request. Any use of trade, firm, or product names is for descriptive purposes only and does not imply endorsement by the U.S. Government.

Funding This work was funded by California Department of Water Resources.

Data availability The data analyzed during the current study are available from the corresponding author on reasonable request.

Declarations

Ethical approval All animal care and handling was approved and followed strict guidelines put forth by the U.S. Fish and Wildlife Service.

Conflict of interest There is no conflict of interest declared in the article.

Financial interests The authors have no relevant financial or non-financial interests to disclose.

References

Adams NS, Plumb JM, Perry RW, Rondorf DW (2014) Performance of a surface bypass structure to enhance juvenile steelhead passage and survival at Lower Granite Dam, Washington. North Am J Fish Manag 34(3):576–594

Brown LR, Bauer ML (2010) Effects of hydrologic infrastructure on flow regimes of California's Central Valley rivers: implications for fish populations. River Res Appl 26(6):751–765

Buchanan RA, Skalski JR, Brandes PL, Fuller A (2013) Route use and survival of juvenile Chinook salmon through the San Joaquin River Delta. North Am J Fish Manag 33(1):216–229

Buchanan R, Brandes P, Marshall M, Nichols K, Ingram J, LaPlante D, Israel J (2016) 2013 South Delta Chinook Salmon survival study. U.S. Fish and Wildlife Service, Pacific Southwest Region, Lodi Fish and Wildlife Office, Lodi, California

Buchanan RA, Brandes PL, Skalski JR (2018) Survival of juvenile fall-run Chinook Salmon through the San Joaquin River delta, California, 2010–2015. North Am J Fish Manag 38(3):663–679

Buchanan RA, Skalski JR (2020) Relating survival of fall-run Chinook Salmon through the San Joaquin Delta to river flow. Environ Biol Fish 103(5):389–410

Buchanan RA, Buttermore E, Israel J (2021) Outmigration survival of a threatened steelhead population through a tidal estuary. Can J Fish Aquat Sci 78(12):1869–1886

Burnham KP, Anderson DR (1998) Practical use of the information-theoretic approach. In Model selection and inference. Springer, New York, NY, pp. 75–117

California Department of Water Resources (2009) DSM2 v8.1.2 Calibration. California Natural Resources Agency. https://data.cnra.ca.gov/dataset/dsm2-v8-1-2-calibration. Accessed 21 Sept 2021

Cavallo B, Gaskill P, Melgo J, Zeug SC (2015) Predicting juvenile Chinook Salmon routing in riverine and tidal channels of a freshwater estuary. Environ Biol Fish 98(6):1571–1582

Chapman ED, Hearn AR, Michel CJ, Ammann AJ, Lindley ST, Thomas MJ, Sandstrom PT, Singer GP, Peterson ML, MacFarlane RB, Klimley AP (2013) Diel movements of out-migrating Chinook salmon (*Oncorhynchus tshawytscha*) and steelhead trout (*Oncorhynchus mykiss*) smolts in the Sacramento/San Joaquin watershed. Environ Biol Fish 96(2):273–286

Evans SD, Adams NS, Rondorf DW, Plumb JM, Ebberts BD (2008) Performance of a prototype surface collector for juvenile salmonids at Bonneville Dam's first powerhouse on the Columbia River, Oregon. River Res Appl 24(7):960–974

Godin G (1972) The analysis of tides. University of Toronto Press, Toronto

Hance DJ, Perry RW, Burau JR, Blake A, Stumpner P, Wang X, Pope A (2020) Combining models of the critical streakline and the cross-sectional distribution of juvenile salmon to predict fish routing at river junctions. San Francisco Estuary and Watershed Science 18(1)

Hayhoe K, Cayan D, Field CB, Frumhoff PC, Maurer EP, Miller NL, Moser SC, Schneider SH, Cahill KN, Cleland EE, Dale L (2004) Emissions pathways, climate change, and impacts on California. Proc Natl Acad Sci 101(34):12422–12427

Jackson C (2011) Multi-state models for panel data: the msm package for R. J Stat Softw 38(1):1–28
Johnson GE, Dauble DD (2006) Surface flow outlets to protect juvenile salmonids passing through hydropower dams. Rev Fish Sci 14(3):213–244
Lennox RJ, Paukert CP, Aarestrup K, Auger-Méthé M, Baumgartner L, Birnie-Gauvin K, Bøe K, Brink K, Brownscombe JW, Chen Y, Davidsen JG (2019) One hundred pressing questions on the future of global fish migration science, conservation, and policy. Front Ecol Evol 7:286
Lindsey JK (2004) Statistical analysis of stochastic processes in time, vol 14. Cambridge University Press, Cambridge
Maurer EP (2007) Uncertainty in hydrologic impacts of climate change in the Sierra Nevada, California, under two emissions scenarios. Clim Change 82(3):309–325
Metcalfe NB, Fraser NH, Burns MD(1998) State–dependent shifts between nocturnal and diurnal activity in salmon. Proc R Soc Lond B Biol Sci 265(1405):1503–1507
Metcalfe NB, Fraser NH, Burns MD (1999) Food availability and the nocturnal vs. diurnal foraging trade-off in juvenile salmon. J Anim Ecol 68(2):371–381
National Research Council (1996) Upstream: salmon and society in the Pacific Northwest. National Academies Press ,Washington
Newman KB, Brandes PL (2010) Hierarchical modeling of juvenile Chinook salmon survival as a function of Sacramento–San Joaquin Delta water exports. North Am J Fish Manag 30(1):157–169
Nichols FH, Cloern JE, Luoma SN, Peterson DH (1986) The modification of an estuary. Science 231(4738):567–573
Perry RW, Brandes PL, Burau JR, Klimley AP, MacFarlane B, Michel C, Skalski JR (2013) Sensitivity of survival to migration routes used by juvenile Chinook salmon to negotiate the Sacramento-San Joaquin River Delta. Environ Biol Fish 96(2):381–392
Perry R, Romine JG, Adams NS, Blake AR, Burau JR, Johnston SV, Liedtke TL (2014) Using a non-physical behavioral barrier to alter migration routing of juvenile chinook salmon in the Sacramento–San Joaquin River delta. River Res Appl 30(2):192–203
Perry RW, Brandes PL, Burau JR, Sandstrom PT, Skalski JR (2015) Effect of tides, river flow, and gate operations on entrainment of juvenile salmon into the interior Sacramento–San Joaquin River Delta. Trans Am Fish Soc 144(3):445–455
Perry RW et al (2018) Flow-mediated effects on travel time, routing, and survival of juvenile Chinook salmon in a spatially complex, tidally forced river delta. Can J Fish Aquat Sci 75(11):1886–1901
Plumb JM, Adams NS, Perry RW, Holbrook CM, Romine JG, Blake AR, Burau JR (2016) Diel activity patterns of juvenile late fall-run Chinook Salmon with implications for operation of a gated water diversion in the Sacramento–San Joaquin River Delta. River Res Appl 32(4):711–720
R Core Team (2021) R: A language and environment for statistical computing. R Foundation for Statistical Computing, Vienna. http://www.R-project.org/
Romine JG, Perry RW, Pope AC, Stumpner P, Liedtke TL, Kumagai KK, Reeves RL (2016) Evaluation of a floating fish guidance structure at a hydrodynamically complex river junction in the Sacramento–San Joaquin River Delta, California, USA. Mar Freshw Res 68(5):878–888
Romine JG, Perry RW, Stumpner PR, Blake AR, Burau JR (2021) Effects of tidally varying river flow on entrainment of juvenile salmon into sutter and steamboat sloughs. San Francisco Estuary and Watershed Science 19(2)
Steel AE, Sandstrom PT, Brandes PL, Klimley AP (2013) Migration route selection of juvenile Chinook salmon at the Delta Cross Channel, and the role of water velocity and individual movement patterns. Environ Biol Fish 96(2):215–224
Thieurmel B, Elmarhraoui A(2019) suncalc: Compute Sun Position, Sunlight Phases, Moon Position and Lunar Phase. R package version 0.5.0. https://CRAN.R-project.org/package=suncalc. Accessed Oct 2021